Southern tropical upper tropospheric zonal ozone wave-1 from SAGE II observations (1985–2002)

Pi-Huan Wang,[1] Jack Fishman,[2] V. Lynn Harvey,[3] and Matthew H. Hitchman[4]

Received 19 May 2005; revised 9 November 2005; accepted 10 January 2006; published 29 April 2006.

[1] Using multiyear data (1985–2002) derived from the second Stratospheric Aerosol and Gas Experiment (SAGE II) and meteorological information (1992–2004) from the United Kingdom Meteorological Office, the present study investigates the seasonal structure of the southern tropical zonal ozone wave-1 in the upper troposphere. By using multiyear near-global ozone profile measurements from the SAGE II satellite instrument, the present study complements the analyses based on data from tropical ozonesonde networks, such as the Southern Hemisphere Additional Ozonesondes (SHADOZ), and from satellite total tropospheric ozone. The seasonal variations in the meridional ozone distributions in the high-ozone longitudinal sector (40°W–60°E) and the low-ozone longitudinal sector (60°E–320°E) are investigated in detail. The results indicate that the southern tropical zonal ozone wave-1 is a year-round feature, with the strongest amplitude occurring in austral spring and weakest in autumn. The influence of the meridional (Hadley) and equatorial (Walker) circulations on the ozone wave-1 is also examined. The analysis suggests that both Hadley and Walker circulations can contribute to the formulation of the ozone wave-1 climatological structure.

Citation: Wang, P.-H., J. Fishman, V. L. Harvey, and M. H. Hitchman (2006), Southern tropical upper tropospheric zonal ozone wave-1 from SAGE II observations (1985–2002), *J. Geophys. Res.*, *111*, D08305, doi:10.1029/2005JD006221.

1. Introduction

[2] Significant advancement of information on the behavior of tropospheric ozone has been made in recent years. It is understood that the troposphere is not just a simple sink for stratospheric ozone. It has its own complex biogenic and anthropogenic ozone sources [e.g., *Fishman et al.*, 1991; *Crutzen*, 1995; *Levy et al.*, 1997; *Wennberg et al.*, 1998]. In fact, tropospheric ozone has complex spatial and temporal features ranging from regional to global and from daily to interannual variations. It is still a great challenge to characterize its behavior [e.g., *Integrated Global Observing Strategy* (*IGOS*), 2004]. The motivation of the present investigation stems from the phenomenon characterized as a zonal wave-1 in the Southern tropical tropospheric ozone column [*Fishman et al.*, 1990; *Shiotani*, 1992] and in the longitudinal distribution of ozone vertical profiles [*Thompson et al.*, 2003], the so-called Tropical Atlantic Paradox [*Thompson et al.*, 2000; *Sauvage et al.*, 2004]. The paradox refers to the higher tropospheric ozone south of the Intertropical Convergence Zone (ITCZ) over the Atlantic during December-January-February when biomass burning is most active north of the ITCZ [*Thompson et al.*, 2003].

[3] *Fishman et al.* [1991] showed that elevated levels of tropospheric ozone over southern Africa and the adjacent eastern tropical South Atlantic Ocean are related to distant biomass burning in Africa. They also pointed out that the agreement between the seasonal cycles of satellite-derived tropospheric ozone data and that of surface CO and CH_4 measurements from biomass burning is not perfect, and other sources, sinks, and transport mechanisms are likely to be responsible for the differences. Since then, considerable effort has been devoted to understanding the mechanisms that lead to this distinctive zonal ozone wave-1 phenomenon [e.g., *Thompson*, 2003, and references therein].

[4] During the NASA Global Tropospheric Experiment (GTE)/Transport and Atmospheric Chemistry Near the Equator–Atlantic (TRACE-A) field experiment (September to October 1992), *Browell et al.* [1996] showed that high ozone was observed in low-altitude biomass burning plumes and in the upper troposphere (UT) where ozone often exceeds 100 ppbv despite low aerosol loadings, indicating possible stratospheric ozone origin. They further showed that biomass burning contributed up to half of the ozone column across the South Atlantic Basin, in qualitative agreement with the analysis of *Olson et al.* [1996], who showed that lower tropospheric ozone (below 600 hPa) contributed up to 60% of the tropospheric ozone column during the TRACE-A field mission. From the TRACE-A experiment, *Pickering et al.* [1996] showed an estimated 25% ozone enhancement in the UT (8–16 km) over the tropical Atlantic, Africa, and Indian Ocean during postcon-

[1]Science and Technology Corporation, Hampton, Virginia, USA.
[2]Science Directorate, NASA Langley Research Center, Hampton, Virginia, USA.
[3]Laboratory for Atmospheric and Space Physics, University of Colorado, Boulder, Colorado, USA.
[4]Atmospheric and Oceanic Sciences, University of Wisconsin, Madison, Wisconsin, USA.

0148-0227/06/2005JD006221

vection, following biomass burning events in eastern Brazil [see also *Garstang et al.*, 1996; *Tyson et al.*, 1997]. In the free troposphere (2–8 km), an ozone enhancement over the tropical Atlantic of about 50% was estimated by *Thompson et al.* [1996]. Clearly, the contribution of biomass burning to the vertical distribution of ozone south of the ITCZ exhibits a high degree of spatial and temporal variability.

[5] Recognizing the potential photochemical and lightning sources of ozone in the troposphere, researchers paid considerable attention to the effect of tropical seasonal biomass burning on the tropospheric ozone distribution. According to a study of the annual tropospheric ozone budget by *Levy et al.* [1997], the UT can be considered as a source region for ozone with the contribution from stratospheric injection (696 Tg/yr) and tropical free tropospheric ozone production (163 Tg/yr), while the main sink of ozone is dry deposition at the surface (−825 Tg/yr) and the CO-CH_4 background boundary layer chemistry (−649 Tg/yr), although boundary layer pollution production generates 686 Tg/yr. On the basis of data from the Measurement of Ozone by Airbus In-Service Aircraft (MOZAIC), *Sauvage et al.* [2004] showed that the northern tropics fires in boreal winter might contribute up to 20% of the global photochemical ozone production. Although the seasonalities of biomass burning and lightning statistics do not match perfectly with the tropical tropospheric ozone amount [*Fishman et al.*, 1991; *Thompson et al.*, 2001, 2003], recent analyses indicate that lightning appears to be a major contributor in the upper tropospheric ozone formation (e.g., *Moxim and Levy* [2000], *Peters et al.* [2002], *Edwards et al.* [2003], *Chatfield et al.* [2004], *Jenkins and Ryu* [2004]; see also the TRACE-A and SAFARI special issue of Journal of Geophysical Research, 98, 1993).

[6] It is worth noting that the SHADOZ ozonesonde profile measurements in 1998–2000 show distinctly different ozone longitude-height distributions during September-October-November (SON) compared to March-April-May (MAM) in the southern tropics [*Thompson et al.*, 2003, Figure 4; see also *Thompson et al.*, 2004, Figure 4]. In addition to much higher ozone in SON than in MAM, the distribution in SON shows regional ozone peaks at 6 km over Ascension (8°S, 18°W) and at 9 km over Reunion (21°S, 53°E), along with a large zonal ozone enhancement in the upper troposphere (UT) above about 12 km, except over Watukosek (8°S, 110°E), where deep convection lofts ozone-poor air into the UT. It appears that the southern tropical ozone enhancement above 12 km is primarily due to ozone influx from the stratosphere [e.g., *Krishnamurti et al.*, 1993, 1996; *Thompson et al.*, 2000; *Chatfield et al.*, 2004], while the regional ozone peaks over Ascension (8°S, 18°W) and Reunion (21°S, 53°E) are mostly due to the influence of seasonal biomass burning and lighting NO.

[7] The presence of stratospheric ozone in the tropical UT (above 14 km and below the lapse-rate tropopause, the so-called tropopause transition layer (TTL)) is also suggested in a recent study by *Folkins et al.* [1999]. The ozonesonde and aircraft measurements obtained during the March 1996 Pacific Exploratory Mission (PEM) tropics A, indicate that ozone mixing ratios usually start increasing toward stratospheric values near 14 km and that there is a transition zone between 14 km and the tropopause, where some fraction of the ozone originated in the stratosphere. This notion of upper tropospheric ozone of stratospheric origin is further supported by tropical data at 10–12 km from the MOZAIC project [*Suhre et al.*, 1997]. *Zachariasse et al.* [2000, 2001] have suggested the important role of stratospheric intrusions associated with the subtropical jet (STJ) in the tropical tropospheric ozone budget.

[8] The objectives of the present study are to investigate the climatological structure of the UT zonal ozone wave-1 in the southern tropics and to explore its large-scale dynamical influence, including meridional (Hadley) and equatorial (Walker) circulation systems, on a seasonal basis, by using ozone profile measurements from the Stratospheric Aerosol and Gas Experiment (SAGE) II. Particular attention is focused on the difference in ozone properties and the meridional circulation between the longitudinal sector with high tropical ozone (40°W–60°E) and the rest of the longitudes (60°E–320°E) with low tropical ozone, in the Southern Hemisphere (SH). The data and methods used in the present study are described in section 2. Properties of the ozone wave-1 derived from SAGE II observations are presented in section 3, followed by interpretation and discussion in section 4. It will be argued that there are significant contributions from both the equatorial Walker circulation and local Hadley circulation in the Atlantic–Indian Ocean sector. The summary, conclusions, and remarks are given in section 5.

2. Data and Analysis

2.1. SAGE II Data Characteristics

[9] The SAGE II sensor aboard the Earth Radiation Budget Satellite (ERBS) has been operating since October 1984. The instrument uses the solar occultation technique to measure stratospheric constituents including aerosols and gaseous species during sunrise and sunset periods, as encountered by the spacecraft [*McCormick*, 1987]. The SAGE II sensor is equipped with seven channels centered at 0.385-, 0.448-, 0.453-, 0.525-, 0.600-, 0.940-, and 1.02-μm wavelengths. The 0.600-μm channel is centered at the peak of the ozone Chappuis band and is used for ozone vertical profile retrieval after removal of the Rayleigh scattering from transmission estimates using meteorological information from the National Center for Environmental Prediction (NCEP) [*Chu et al.*, 1989].

[10] Although SAGE II is not optimally designed for tropospheric monitoring, the four longer-wavelength channels frequently sample into the troposphere [*Wang*, 1994; *Wang et al.*, 1994; *Wang et al.*, 1998a]. How deep the SAGE II instrument can measure into the troposphere depends on the altitude of cloud presence. There are two general types of clouds that can be distinguished in SAGE II observations, namely, opaque clouds (OC) and subvisible clouds (SVC) [*Wang et al.*, 1996; *Wang et al.*, 2001]. The presence of opaque clouds terminates the SAGE II profiling. Unlike the opaque clouds, the extinction coefficient at 0.525 and 1.02 μm can be measured in the presence of subvisible clouds, but they complicate the ozone retrieval from the transmission data at 0.600 μm. For this reason, SAGE II data with cloud presence are removed for the present investigation by using a two-wavelength method for SAGE II cloud identification developed by *Kent et al.* [1993]. In addition, as with the presence of clouds, high aerosol

loadings immediately following major volcanic eruptions, such as the June 1991 Mt. Pinatubo event, also make the SAGE II data retrieval less reliable [*Cunnold et al.*, 1996]. As a result, the SAGE II retrievals between June 1991 and December 1993 are excluded from the present analysis.

[11] The SAGE II tropospheric ozone data quality has been analyzed by *Wang et al.* [2002]. SAGE II ozone data show excellent agreement with ozonesondes in the stratosphere above 19 km, where differences are less than 1%. Differences increase to about 20% at the tropopause ($\sim$16 km) and into the upper troposphere. Below $\sim$11 km, differences increase to 50% and at 5 km they are 90%. Despite the low ozone bias, a zonal ozone wave-1 is observed in the southern tropical upper troposphere when many years of SAGE II ozone data are combined. The climatological structure of this ozone wave-1 and its seasonal variability will be examined in section 3.

2.2. Large-Scale Circulation Derivation

[12] Naturally, transport processes must play an important role in ozone distributions in the upper troposphere, where the ozone lifetime is about 1 month [*Thompson et al.*, 2004]. To explore the influence of large-scale dynamics on the southern tropical ozone distribution in a climatological perspective, we investigate the relationship between the ozone distribution and transport system associated with the equatorial (Walker) and meridional (Hadley) circulations.

2.2.1. Mean Meridional Circulation Model

[13] Because clouds are a proxy for the large-scale circulation [e.g., *Webster*, 1983; *Wang*, 1994], *Wang et al.* [1998a] presented a simple and robust cloud and circulation interaction model (CCIM) for diagnosis of the mean meridional circulation based on SAGE II tropospheric measurement statistics. The model assumes that the vertical velocity, w, of the zonal mean tropospheric circulation is a linear function of the departure of the measurement frequency, Δf_m, from the associated global average, that is,

$$w(z,\theta) = -\kappa \Delta f_m(z,\theta), \tag{1}$$

where θ indicates the latitude, z indicates the altitude, and κ is a proportionality constant. In practice, the constant κ serves as a calibrational coefficient in an experimental sense. It relates the vertical velocity distribution to the cloud field and thus quantifies their interaction. A value of 8.3×10^{-5} m/s [*Wang et al.*, 1998a] was determined based on a combination of the vertical circulation climatologies of *Schubert et al.* [1990], *Peixoto and Oort* [1992], and *Trenberth* [1992]. The continuity equation is then used to infer the meridional velocity field from the vertical circulation. Readers are referred to *Wang et al.* [1998a] for a more detailed presentation of the CCIM. This CCIM has been employed in the study of the impact of the El Niño 1997/1998 on the mean meridional circulation [*Wang et al.*, 2003]. As we will see in section 4, the CCIM provides supporting evidence for the importance of the Hadley and Walker circulations to the formulation of the southern tropical zonal ozone wave-1.

2.2.2. Equatorial (Walker) Circulation

[14] The vertical velocity distribution can be calculated from the cloud distribution by using equation (1). In this case, the measurement frequency, Δf_m, used for vertical velocity calculation is the departure from the tropical zonal mean. However, a full CCIM for determining the Walker circulation is presently not available. This is due mainly to insufficient boundary condition and constraint for determining the zonal wind field from the continuity equation. To make the analysis tractable, we have incorporated the United Kingdom (UK) meteorological data, i.e., zonal wind (from 1992 to 2004) [*Swinbank and O'Neill*, 1994; *Lorenc et al.*, 2000], into the seasonal climatology of the equatorial circulation in the southern tropics. As will be shown in section 4, the derived equatorial circulation pattern is qualitatively related to the seasonal behavior of the ozone wave-1.

3. Results

3.1. Zonal Structure

[15] The longitude-height cross section of the multiyear (1985–2002) mean ozone distribution for the latitudinal band between 20°S and the equator is displayed in Figure 1. The ozone concentration in the 4–11 km layer is higher than average in the longitudinal sector between about 40°W and 60°E in the UT, with the center located at about 20°E. This distinct zonal ozone distribution is directly related to the southern tropical zonal ozone wave-1 feature reported by *Thompson* [2003; see also *Thompson et al.*, 2003] based on data between 1998 and 2000 derived from nine ozonesonde stations in the southern tropics. Note that near 15 km, ozone concentrations are higher in the band 180°W–50°E, and that the vertical gradient is such that the ozone mixing ratio increases toward the stratosphere. These features give an important clue as to the likely stratospheric origin of this ozone anomaly.

[16] Figure 2 presents the seasonal evolution of the ozone wave-1. The level of the southern tropical ozone in the longitudinal sector 40°W–60°E is generally higher than that in the longitudinal sector 60°E–320°E all the year round. The amplitude of the ozone wave-1 is the smallest during austral autumn (MAM). It then greatly intensifies during June-July-August (JJA), and continues into SON. During December-January-February (DJF), the ozone wave-1 is weaker but clearly maintained. Note the eastward shift of the ozone maximum in the UT over Africa during MAM–SON. Interestingly, an eastward shift of the Tropical Tropospheric Ozone Column (TTOC) maximum during DJF–JJA has been shown in the MOZAIC ozone observations [*Sauvage et al.*, 2004].

3.2. Ozone Wave-1 at Constant Height

[17] Seasonal variations of the ozone distribution at 10 km are displayed in Figure 3. The blank areas result from missing data, presumably due to frequent opaque clouds at 10 km as they occur predominantly in the tropics (especially over the tropical western Pacific). Generally, the ozone concentration increases poleward at mid and high latitudes, along with large-scale zonal asymmetries at low latitudes. The low ozone values over Micronesia, northern South America, and western central Africa are indicative of large-scale features associated with the ascending branch of the Hadley and Walker circulation cells. (According to *Webster* [1983], the tropical Pacific circulation with rising motion in the west and sinking motion in the east along with

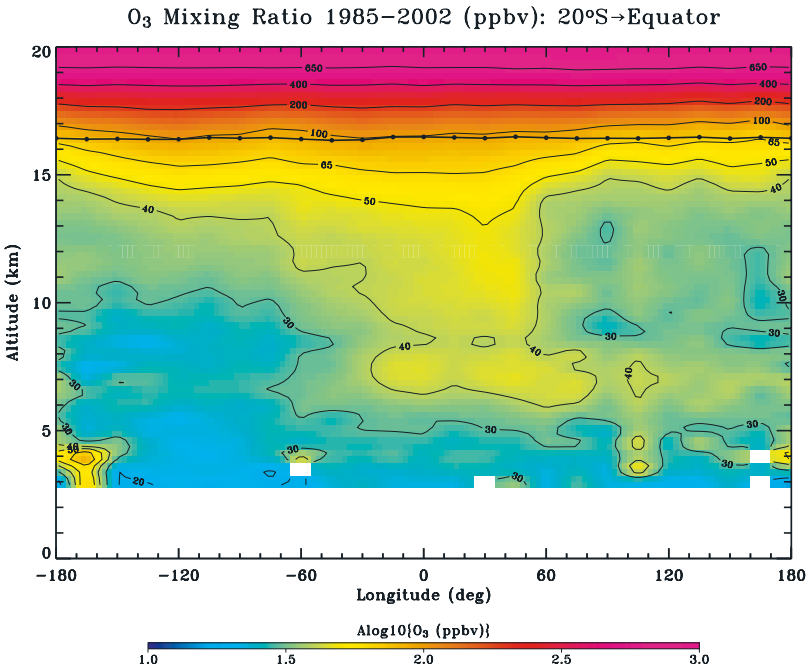

Figure 1. Multiyear (1985–2002) mean longitude-altitude ozone mixing ratio distribution for the southern tropics (20°S–equator). The ozone concentrations are color-coded and are contoured at 30, 40, 50, 65, 100, 200, 400, and 650 ppbv. Dots indicate the tropopause location.

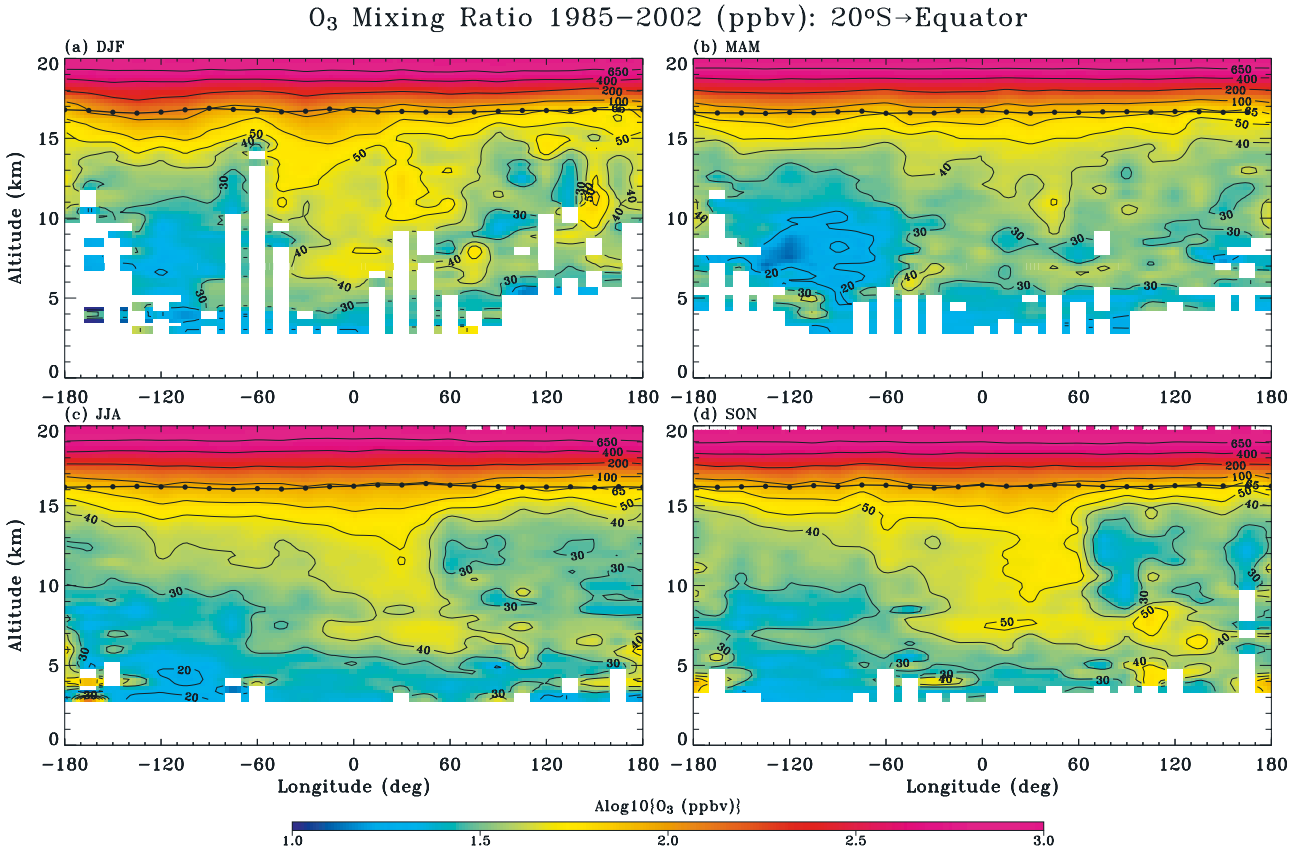

Figure 2. Multiyear (1985–2002) seasonal mean longitude-altitude ozone mixing ratio distribution for the southern tropics (20°S–equator). The ozone concentrations are color-coded and are contoured at 30, 40, 50, 70, 100, 200, 400, and 650 ppbv. Dots indicate the tropopause location.

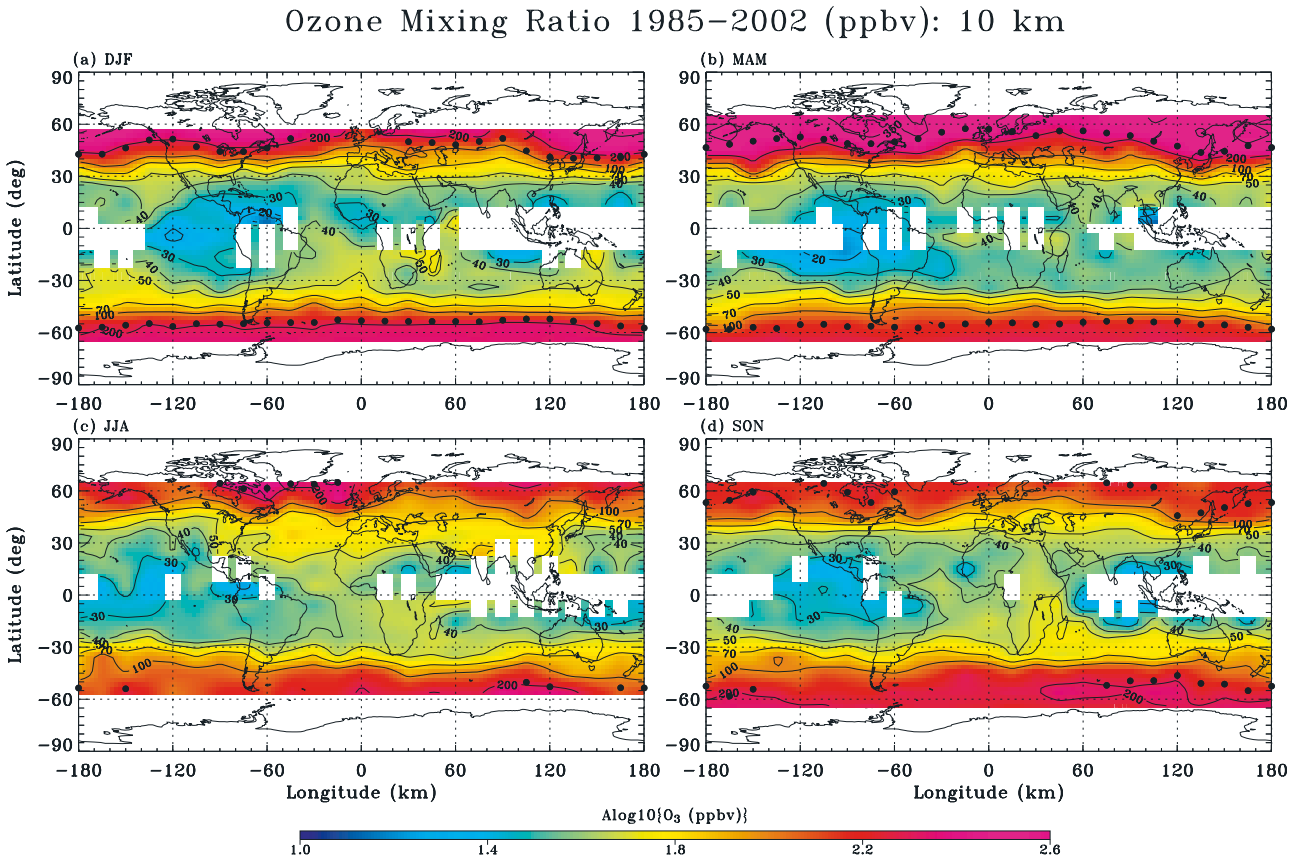

Figure 3. Longitude-latitude distribution of multiyear (1985–2002) seasonal mean ozone mixing at 10 km. The ozone concentrations are color-coded and are contoured at 30, 40, 50, 70, 100, 200, and 350 ppbv. Dots indicate the tropopause location.

a westward flow at low levels and an eastward flow in the UT is referred to as the Walker circulation.) Note that the southern tropical ozone concentration between 40°W and 60°E is notably higher than at other longitudes, and the difference is the greatest in SON and the weakest in MAM, a feature that is directly related to the southern tropical zonal ozone wave-1 phenomenon.

3.3. Meridional Structure

[18] The near global coverage of the SAGE II ozone profile measurements allows us to further explore the meridional extent of the zonal ozone wave-1 structure in the UT. In doing this, we compare the seasonal characteristics of the ozone meridional distributions in 40°W–60°E with those in 60°E–320°E. The results are presented in Figure 4. It is noted that because of the low ozone bias of the SAGE II data in the troposphere below 10 km, caution must be exercised regarding the detail in the lower troposphere (LT) in Figure 4.

3.3.1. Between 40°W and 60°E

[19] During DJF, there is a distinct hemispheric asymmetry in the ozone distribution in the UT, with much higher ozone in the SH than in the Northern Hemisphere (NH). During MAM, the ozone concentration is reduced in the SH, while the ozone concentration increases at northern midlatitudes, resulting in a more or less symmetric meridional ozone distribution (Figure 4b). In JJA, the ozone loading exhibits significant enhancement at southern low latitudes in the UT (Figure 4c). Interestingly, the ozone concentration in the northern subtropics reveals an even larger increase. The UT ozone in the northern extratropics sharply reduces in SON (Figure 4d). In contrast, the ozone in the southern UT continues to increase in SON. Note the spread of ozone between 40 and 50 ppbv across the equator at altitudes 10 to 13 km. This feature appears to indicate possible cross-equatorial ozone transport along isentropic surfaces centered at 345 K as ozone increases in the SH and decreases in the NH during the seasonal transition from JJA to SON. The ozone concentration declines slightly from SON to DJF in the southern UT (Figures 4a and 4d).

3.3.2. Between 60°E and 320°E

[20] The ozone concentration is higher in the SH than in the NH during DJF (Figure 4e) similar to the situation in the band 40°W–60°E (Figure 4a). However, at southern low latitudes, the ozone concentration in the middle troposphere is generally lower in 60°E–320°E than in 40°W–60°E. During MAM, the ozone distribution in 60°E–320°E is similar to that in 40°W–60°E, except at low latitudes (Figures 4b and 4f), where ozone is very low, likely due to the presence of stronger convection there [e.g., *Folkins and Martin*, 2005].

[21] By JJA, the ozone concentration in 60°E–320°E is higher in the northern UT than in the southern UT (Figure 4g). Compared to the ozone in 40°W–60°E, the

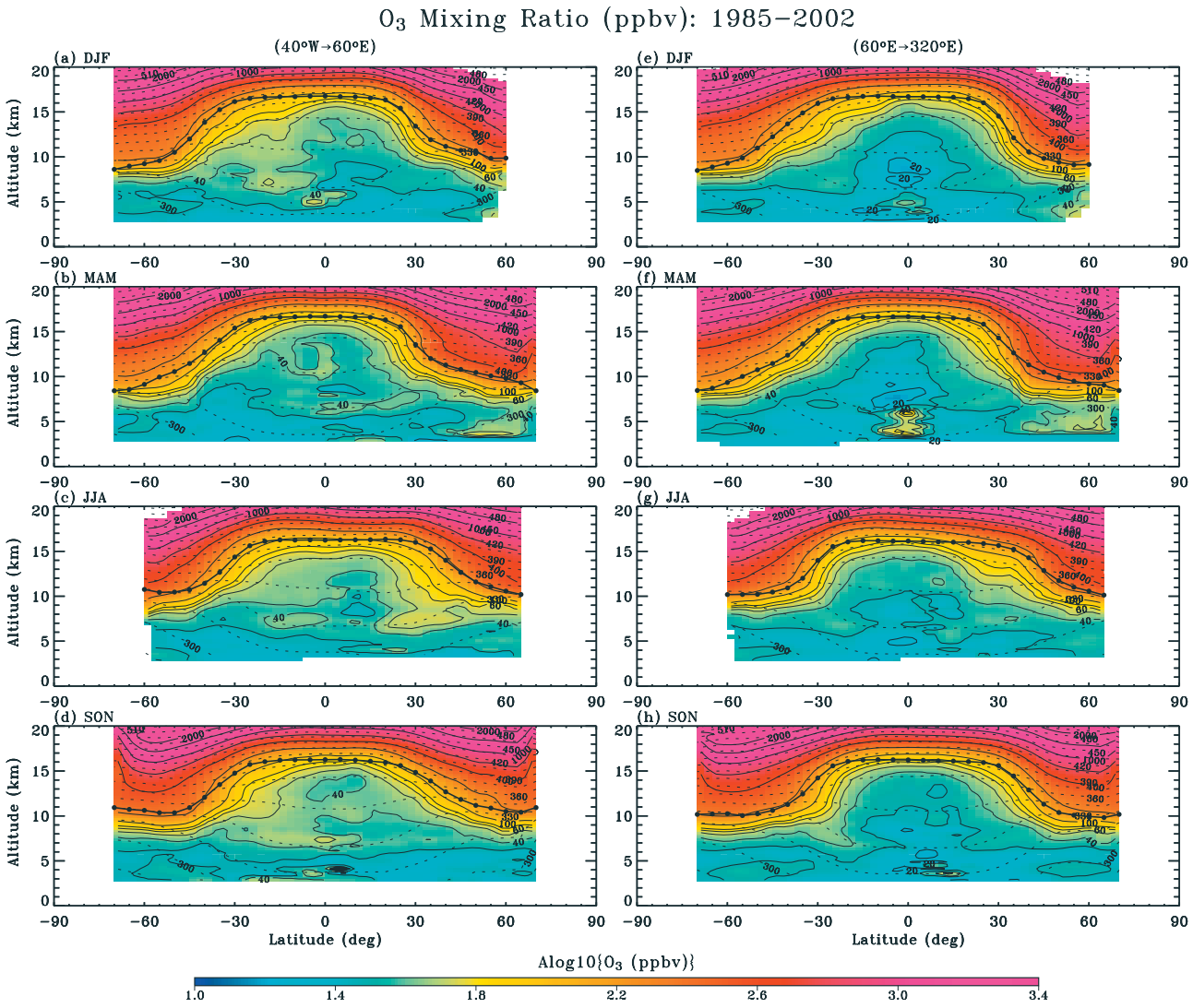

Figure 4. Comparison of the seasonal latitude-altitude ozone mixing ratio distribution in the longitudinal sector (left) 40°W–60°E with that in the longitudinal sector (right) 60°E–320°E. The ozone concentrations are color-coded and are contoured at 30, 40, 50, 60, 70, 100, 200, 400, 650, 1000, 1500, 2000, and 3000 ppbv. The dashed lines indicate the isentropic contour with an increment of 15 K beginning at 270 K. The thick line with dots indicates the location of the tropopause.

ozone in 60°E–320°E is smaller in the UT, particularly at midlatitudes (Figures 4c and 4g). During SON, ozone decreases in the northern UT, while it slightly increases in the southern UT (Figure 4h). In comparison to the UT ozone in 40°W–60°E, the ozone concentration in 60°E–320°E appears to be about the same in the NH, but it is much lower in the SH (Figures 4d and 4h). As will be shown, the seasonal variations of these meridional ozone distributions are related to the strength of the Hadley circulation.

4. Discussion

[22] From the analysis presented in the preceding subsections, it is evident that in the low-latitude UT, the seasonal ozone variations in 40°W–60°E are different from those in 60°E–320°E. In 60°E–320°E, the UT ozone distribution in the SH exhibits a seasonal behavior generally similar to that in the NH, with the ozone concentration minimizing during JJA and peaking in DJF (Figures 4e–4h). In 40°W–60°E, on the other hand, persistent ozone enhancement is observed from MAM through SON, contrasting with the seasonal ozone variation in the NH, that minimizes in DJF and peaks in JJA (Figures 4a–4d). The distinct, different seasonal ozone behavior in the UT between these two longitudinal sectors suggests that they are influenced differently by ozone-controlling mechanisms.

[23] The ozone enhancement in the northern low-latitude UT during JJA (Figure 4g) appears to be consistent with the general notion that the large-scale descent associated with the downward branch of the Brewer-Dobson circulation occurs during winter and spring at northern high latitudes [*Rosenlof et al.*, 1997]. This circulation brings ozone-rich air into the lowermost stratosphere. From there, the ozone-rich air spreads to lower latitudes and into the troposphere via quasi-isentropic processes associated with breaking baroclinic synoptic disturbances in spring and monsoon

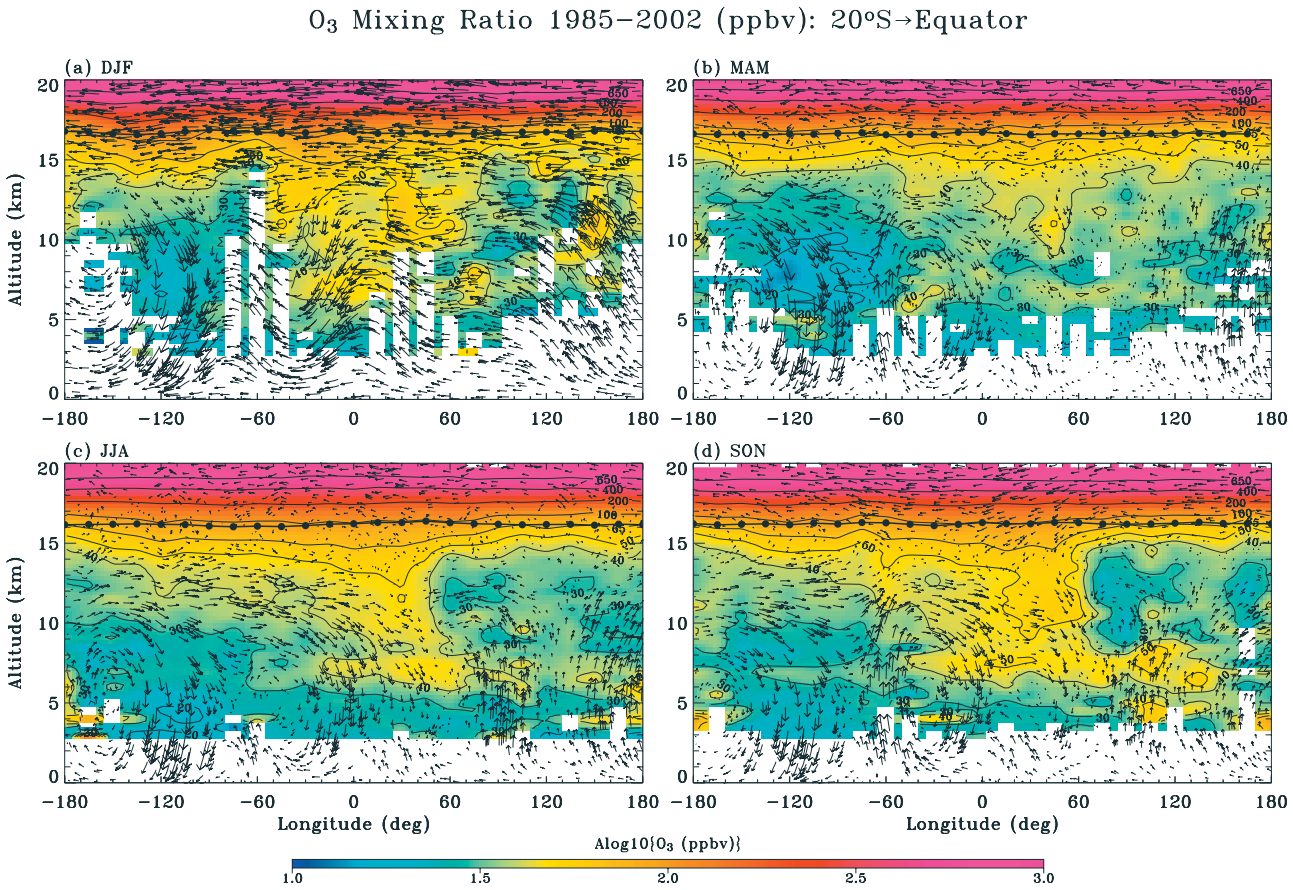

Figure 5. A superposition plot of the longitude-altitude ozone distribution (Figure 2) and the Walker circulation in the southern tropics (20°S–equator). The thick line with dots indicates the location of the tropopause. The vertical velocity is scaled by 2000 for proper vector plot.

activities in summer [e.g., *Hitchman et al.*, 1994; *Chen*, 1995; *Dunkerton*, 1995; *Wang et al.*, 1998b; *Postel and Hitchman*, 1999; *Jing et al.*, 2004; M. H. Hitchman et al., On the relationship between the Tibetan high and the ozone croissant, manuscript in preparation for *Geophysical Research Letters*, 2006, hereinafter referred to as Hitchman et al., manuscript in preparation, 2006]. In the SH on the other hand, the seasonal ozone variations in the tropical UT appear to be due to different circulation patterns and more involved contributions from photochemical ozone production by biomass burning and lightning formation of ozone precursors [e.g., *Berntsen and Isaksen*, 1997; *Levy et al.*, 1997; *Wennberg et al.*, 1998; *Wang et al.*, 1998c].

[24] In the present study, we explore the relationship between the ozone wave-1 phenomenon and the large-scale dynamical systems, including the equatorial (Walker) and meridional (Hadley) circulations. In the tropical UT, ozone accumulation takes place mainly through stratospheric ozone intrusion and photochemical ozone production. As the background ozone increases with altitude, the upward branch of the Hadley and Walker circulations brings ozone-poor air into the tropical UT from lower altitudes. The effect of the poleward branch of the Hadley circulation is to transport ozone from the tropical UT to middle and high latitudes. Thus the Hadley circulation tends to slow down ozone accumulation in the tropical UT. In the case of the Walker circulation, the downward branch tends to bring ozone-rich air from the uppermost troposphere into the middle and lower troposphere. Their influence on the ozone wave-1 phenomenon in the UT will be examined in this section, with special attention on the Hadley circulation and the meridional ozone distribution in 40°W–60°E and 60°E–320°E.

4.1. Walker Circulation

[25] The seasonal distributions of ozone mixing ratio, zonal wind derived from the UK Met Office data, and vertical wind derived from equation (1) averaged in the band 20°S-equator are shown in Figure 5. These circulation patterns agree fairly well with other estimates of zonal circulations in the tropics, e.g., *Newell et al.* [1974]. As described by *Krishnamurti et al.* [1996], a salient aspect is the year-round descent in the band 40°W–60°E. Descending airflow in the South Atlantic-Indian Ocean sector appears to increase from MAM through JJA, with persistent descent into SON. Note the downward-eastward extension of high-ozone amounts during JJA and SON, consistent with the idea that ozone diffusing out of the midlatitude lower stratospheric ozone croissant centered south of Australia is contributing to the wave-one ozone maximum in 40°W–60°E (Hitchman et al., manuscript in preparation, 2006). Thus the derived walker circulation supports contributions to the upper tropospheric ozone wave-1 from the stratosphere, with seasonal variations consistent with ob-

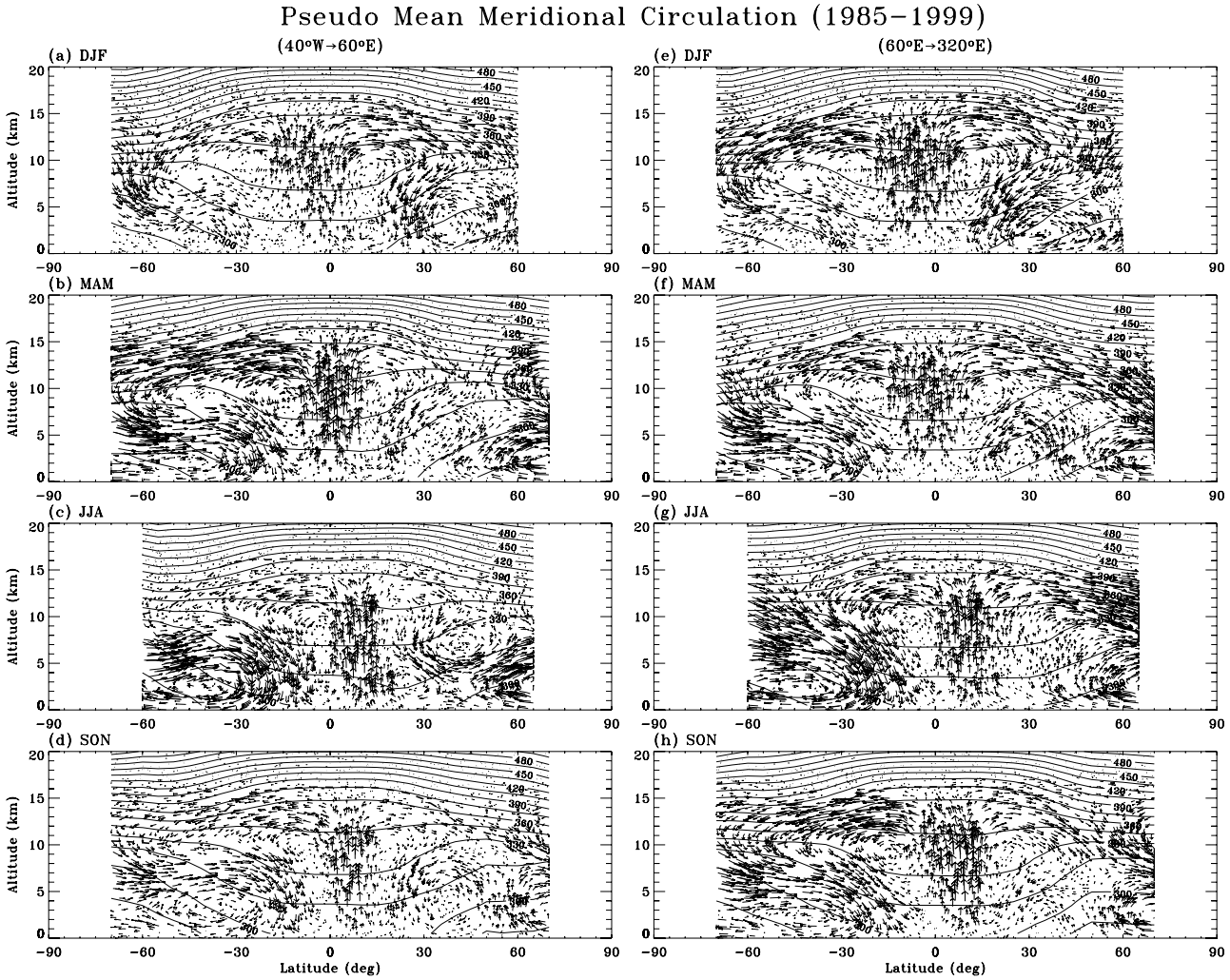

Figure 6. Comparison of the seasonal pseudo-mean meridional circulation in the longitudinal sector (left) 40°W–60°E with that in the longitudinal sector (right) 60°E–320°E. The solid lines indicate the isentropic contour with an increment of 15 K beginning at 270 K. The thick dashed line indicates the location of the tropopause. The vertical velocity is scaled by 2000 for proper vector plot.

served ozone variations. Note the rich ozone layer centered at about 7.5 km in region 60°W–120°E during SON. Note also that the maximum near 100°E is associated with strong ascending air flow. We speculate that this ozone maximum is related to in situ sources due to pollution, biomass burning, and lightning. The maximum over 10°E, on the other hand, is associated with strong descending flow. This feature suggests the possible influence of ozone from higher altitudes.

4.2. Hadley Circulation

[26] The seasonal CCIM circulation patterns for 40°W–60°E and 60°E–320°E are presented in Figure 6. It is noted that the present circulation calculation treats the SAGE II mean measurement frequency for 40°W–60°E as well as for 60°E–320°E as if they are zonal means. For this reason they are referred to as pseudo mean meridional circulations (PMMC).

4.2.1. Between 40°W and 60°E

[27] During DJF, the pattern of the PMMC exhibits a dominant direct circulation cell in the SH. In the NH, the PMMC pattern features a direct cell at low latitudes along with an indirect circulation cell at middle and high latitudes (Figure 6a). The downward-equatorward airflow at northern high latitudes tends to bring ozone-rich air across the tropopause from the lowermost stratosphere into the UT, consistent with high ozone near 30°N in Figure 4a. Note that the poleward branch of the Hadley circulation in the UT is weaker in the SH than in the NH. This weaker poleward circulation combined with the stronger photochemical ozone production in the SH than in the NH during DJF appears to be the reason for the higher UT ozone concentration in the SH than in the NH (Figure 4a).

[28] The PMMC in the SH intensifies in MAM (Figure 6b). This change in the Hadley circulation together with declining photochemical production from DJF to MAM in the SH is consistent with the decreased ozone concentration in the southern tropical UT during MAM (Figure 4b). In the NH, the PMMC away from the tropics declines in MAM. This weakened PMMC together with the enhanced production during MAM is likely the cause of the mild ozone increase just below the tropopause at the northern

midlatitudes. Interestingly, the downward-equatorward flow (Figure 6b) apparently is responsible for the extension of ozone-rich air from the UT near 40°N to about 6–7 km at northern low latitudes, following more or less the 330 K potential temperature surface (Figure 4b).

[29] The poleward branches of the PMMC decline in JJA (Figure 6c). This situation favors ozone accumulation in the low-latitude UT via stratospheric ozone injection and photochemical production. Indeed, ozone concentration in the UT is much higher in JJA than in MAM. Particularly, the northward shift of the center of low ozone values in the tropics (Figure 4c) is very consistent with the northward shift of the tropical ascending branch of the PMMC shown in Figure 6c. Note that the sinking branch near 30°N (Figure 6c) creates a plume of enhanced ozone down to 6 km (Figure 4c). In the SH, the vigorous downward-equatorial flow in the subtropics (Figure 6c) contributes to enhanced ozone (Figure 4c). The PMMC appears further weakened in SON, particularly in the tropics (Figure 6d). The combined seasonal changes of the weakened Hadley circulation and the strengthened photochemical production from JJA to SON in the SH are likely responsible for the ozone wave-1 peak in the southern tropical UT during SON (Figure 4d).

4.2.2. Between 60°E and 320°E

[30] During DJF, the poleward Hadley circulation is stronger in the SH than in the NH (Figure 6e). In addition, the upward branch of the Hadley circulation is centered at 12°S. Therefore one would expect less ozone in the SH than in the NH in the UT. Furthermore, the strong downward-equatorward flow at northern high latitudes would also tend to increase the ozone level in the northern UT. However, observations (Figure 4e) show just the opposite ozone distributions with higher UT ozone in the SH than in the NH (Figure 4e). This feature strongly suggests the important role of photochemical production in the low-latitude UT. The PMMC in 60°E–320°E is quite different from that in 40°W–60°E (Figures 6a and 6e). The circulation is more intense in 60°E–320°E (Figure 6e) than in 40°W–60°E (Figure 6a). These different PMMC patterns explain the relatively lower ozone in the tropics and at southern low latitudes, and the slightly higher ozone in the northern extratropics in 60°E–320°E than in 40°W–60°E in the UT (Figures 4a and 4e).

[31] During MAM, the tropospheric PMMC in 60°E–320°E is more or less similar to that in 40°W–60°E in the UT, except at low latitudes, where the tropical ascending circulation in 60°E–320°E (Figure 6f) is broader than in 40°W–60°E (Figure 6b). This feature is likely the reason for the ozone values being lower in 60°E–320°E than in 40°W–60°E in the tropical UT (Figures 4b and 4f).

[32] In JJA, the circulation pattern (Figure 6g) reveals significant seasonal changes from that in MAM (Figure 6f). The entire Northern Hemisphere in 60°E–320°E seems under the influence of a single large Hadley circulation cell. In the SH, the poleward branch of the Hadley circulation turns around at midlatitudes (Figure 6g), instead of at high latitudes as shown in MAM (Figure 6f). In fact, the PMMC in the SH (Figure 6g) generally mirrors that in the NH during DJF (Figure 6e). Compared with the PMMC in 40°W–60°E, the PMMC in 60°E–320°E is stronger in the UT. Thus one would expect lower ozone values in 60°E–320°E than in 40°W–60°E in the southern tropical UT. This is exactly what is observed in the ozone distributions (Figures 4c and 4g).

[33] The predominant northern Hadley circulation cell in JJA declines in SON (Figure 6h). Concurrently, the poleward Hadley circulation at southern midlatitudes intensifies in the UT. This seasonal PMMC evolution in the UT, together with the weakened photochemical production in the NH and strengthened production in the SH during this time of the year, leads to a more or less similar ozone distribution between the NH and the SH in SON (Figure 4h). In comparison, the PMMC in 60°E–320°E (Figure 6h) is much stronger than that in 40°W–60°E (Figure 6d) in the UT. This stronger UT PMMC in 60°E–320°E is indeed in accord with the relatively lower UT ozone in this sector than in 40°W–60°E during SON (Figures 4d and 4g).

[34] To facilitate the discernment of the relationship between the Hadley circulation and the tropical ozone distributions in the low-latitude UT, the derived seasonal PMMC is superimposed on the seasonal ozone altitude-latitude distributions in Figure 7. The negative correlation between the Hadley circulation and ozone concentration in the low-latitude UT is clearly shown in the contrast between the circulation pattern and ozone distributions during DJF (Figure 7a) and those during MAM (Figure 7b) in the longitudinal sector 40°W–60°E. In addition, the predominant transport effect of the Hadley circulation on the ozone distribution at middle and high latitudes is particularly evident in the longitudinal sector 60°E–320°W in the NH during DJF (Figure 7c) and in the SH during JJA (Figure 7d).

5. Summary, Conclusions, and Remarks

[35] On the basis of multiyear (1985–2002) SAGE II measurements and meteorological information (1992–2004) from the United Kingdom Meteorological Office, the present study investigates the seasonal climatology of the southern tropical zonal ozone wave-1 phenomenon in the UT. The results indicate that the southern tropical ozone mixing ratios in 40°W–60°E are higher than those in 60°E–320°E all year long. The seasonal variation of this ozone wave-1 phenomenon is such that it is strongest in SON and is weakest in MAM. Thus the UT southern tropical zonal wave-1 derived from the SAGE II satellite measurements is in qualitative agreement with the SHADOZ ozonesonde profile data analyses [e.g., *Thompson et al.*, 2003].

[36] Furthermore, we have explored the relationship between the ozone wave-1 phenomenon and large-scale dynamics, including the equatorial (Walker) and meridional (Hadley) circulation systems on a seasonal climatological basis. The cloud-circulation interaction model developed by *Wang et al.* [1998a] is adopted in the present study. It is shown that the high ozone longitudinal sector (40°W–60°E) is associated with year-round tropical descending Walker circulation, except in DJF, and that the descending flow is the strongest during SON. In the case of the Hadley circulation, the results of the present analysis indicate that the ozone wave-1 structure is related to the year-round weaker upward and poleward Hadley circulation in 40°W–60°E than in 60°E–320°E in the southern tropics, except during MAM. The strongest ozone wave-1 in SON is

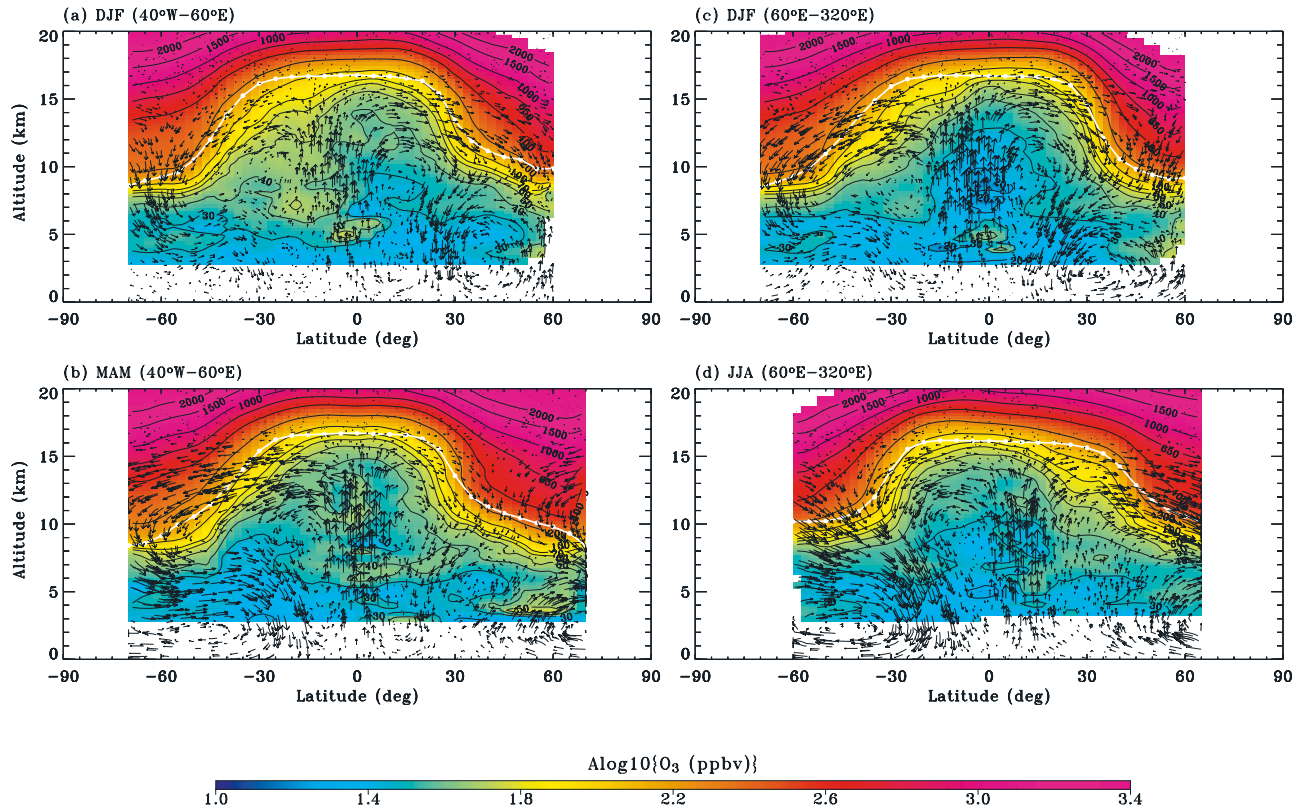

Figure 7. A superposition plot of the latitude-altitude ozone distribution and the pseudo mean meridional circulation in 40°W–60°E for the season (a) DJF and (b) MAM and in 60°E–320°E for (c) DJF and (d) JJA. The ozone concentrations are color-coded and are contoured at 30, 40, 50, 60, 70, 100, 200, 350, 500, 700, and 1000 ppbv. The thick white line with dots indicates the tropopause location.

possibly the result of the weakest tropical upward and poleward Hadley circulation in 40°W–60°E during that time of year. Thus the seasonal variation of the Walker and Hadley circulations can contribute to the formation of the southern tropical zonal ozone wave-1 structure, complementing existing analyses.

[37] As indicated in the article by *Wang et al.* [1998a], the derived mean meridional circulation, according to the large-scale cloud-circulation interaction model, differs distinctly from the conventional Eulerian mean circulation. By adopting this cloud-circulation interaction model, the present study brings out the seasonal effect of the Hadley and Walker circulations on the development of the southern tropical zonal ozone wave-1 phenomenon in the UT. It further illustrates the robust nature of the model and the intimate relationship between the tropospheric large-scale cloud distribution and circulation characteristics.

[38] The results from the present study of the UT ozone seasonal climatology suggest a delicate balance between stratospheric ozone injections, in situ background, biomass-burning, and lightning-related photochemical ozone production, and ozone transport via large-scale circulation in the tropical UT. No attempt is given in the present study to explore the precise sources and sinks of the elevated upper tropospheric ozone. Instead, it presents large-scale seasonal ozone properties in the UT with a focus on the southern tropical zonal ozone wave-1, based on multiyear (1985–2002) ozone profile measurements from the SAGE II satellite instrument. In addition, a qualitative exploration of the relationship between the seasonal behavior of the ozone wave-1 and seasonal variations of the Hadley and Walker circulation systems is presented. It is noted that the large-scale transport in the tropical UT is generally three-dimensional in nature and that the meridional (Hadley) and equatorial (Walker) circulation systems are likely to interact with each other. Thus the study of their relationship to the ozone wave-1 phenomenon separately is not perfect. In addition, the partition of the tropospheric mean meridional circulation into two different longitudinal sectors is perhaps a treatment of the three-dimensional characteristics of the tropospheric dynamics in its crudest fashion. In light of the importance of the tropical tropospheric ozone to air quality and climate, it is a desirable goal to quantify contributions to the southern tropical zonal ozone wave-1 phenomenon using a reliable global chemical transport model (GCTM) in the future.

[39] **Acknowledgments.** The authors would like to thank two anonymous reviewers for their helpful and constructive suggestions and comments. P.-H. Wang is supported by the NASA SOSST program under contract NAS1-02058. The SAGE II data are obtained from the Atmospheric Science Data Center at the NASA Langley Research Center. We would like to thank colleagues at the Met Office for producing the stratospheric assimilated data set. We are grateful to the British Atmospheric Data Centre for providing us with access to the UK MetO data.

References

Berntsen, T. K., and I. S. A. Isaksen (1997), A global three-dimensional chemical transport model for the troposphere: 1. Model description and CO and ozone results, *J. Geophys. Res.*, *102*, 21,239–21,280.

Browell, E. V., et al. (1996), Ozone and aerosol distributions and air mass characteristics over the South Atlantic basin during the burning season, *J. Geophy. Res.*, *101*, 24,043–24,068.

Chatfield, R. B., H. Guan, A. M. Thompson, and J. C. Witte (2004), Convective lofting links Indian Ocean air pollution to paradoxical South Atlantic ozone maxima, *Geophys. Res. Lett.*, *31*, L06103, doi:10.1029/2003GL018866.

Chen, P. (1995), Isentropic cross-tropopause mass exchange in the extratropics, *J. Geophy. Res.*, *100*, 16,661–16,673.

Chu, W. P., M. P. McCormick, J. Lenoble, C. Brogniez, and P. Pruvost (1989), SAGE II inversion algorithm, *J. Geophy. Res.*, *94*, 8339–8351.

Crutzen, P. J. (1995), Ozone in the troposphere, in *Composition, Chemistry, and Climate of the Atmosphere*, edited by H. B. Singh, pp. 349–393, Van Nostrand Reinhold, Hoboken, N. J.

Cunnold, D. M., L. Froidevaux, J. Russel, B. Connor, and A. Roche (1996), An overview of UARS ozone validation based primarily on intercomparisons among UARS and SAGE II measurements, *J. Geophy. Res.*, *101*, 10,335–10,350.

Dunkerton, T. J. (1995), Evidence of meridional motion in the summer lower stratosphere adjacent to monsoon regions, *J. Geophy. Res.*, *100*, 16,675–16,688.

Edwards, D. P., et al. (2003), Tropospheric ozone over the Atlantic: A satellite perspective, *J. Geophys. Res.*, *108*(D8), 4237, doi:10.1029/2002JD002927.

Fishman, J., C. E. Watson, J. C. Larson, and J. A. Logan (1990), Distribution of tropospheric ozone determined from satellite data, *J. Geophy. Res.*, *95*, 3599–3617.

Fishman, J., K. Fakhruzzaman, B. Cros, and D. Nganga (1991), Identification of widespread pollution in the southern hemisphere deduced from satellite analyses, *Science*, *252*, 1693–1696.

Folkins, I., and R. V. Martin (2005), The vertical structure of tropical convection and its impact on the budgets of water vapor and ozone, *J. Atmos. Sci.*, *62*, 1560–1573.

Folkins, I., M. Loewenstein, J. Podolske, S. J. Oltmans, and M. Proffitt (1999), A barrier to vertical mixing at 14 km in the tropics: Evidence from ozonesondes and aircraft measurements, *J. Geophy. Res.*, *104*, 22,095–22,102.

Garstang, M., P. D. Tyson, R. J. Swap, M. Edwards, P. Kallberg, and J. A. Lindesay (1996), Horizontal and vertical transport of air over southern Africa, *J. Geophy. Res.*, *101*, 23,721–23,736.

Hitchman, M. H., M. McKay, and C. R. Trepte (1994), A climatology of stratospheric aerosol, *J. Geophys. Res.*, *99*, 20,689–20,700.

Integrated Global Observing Strategy (IGOS) (2004), *An Integrated Global Atmospheric Chemistry Observation Theme, ESA SP-1282*, 54 pp., Eur. Space Agency, Paris.

Jenkins, G. S., and J.-H. Ryu (2004), Space-borne observations link the tropical atlantic ozone maximum and paradox to lightning, *Atmos. Chem. Phys.*, *4*, 361–375.

Jing, P., D. M. Cunnold, H. J. Wang, and E.-S. Yang (2004), Isentropic cross-tropopause ozone transport in the northern hemisphere, *J. Atmos. Sci.*, *61*, 1068–1078.

Kent, G. S., D. M. Winker, M. T. Osborn, M. P. McCormick, and K. M. Skeens (1993), A model for the separation of cloud and aerosol in SAGE II occultation data, *J. Geophy. Res.*, *98*, 20,725–20,735.

Krishnamurti, T. N., H. E. Fuelberg, M. C. Sinha, D. Oosterhof, E. L. Bensman, and V. B. Kumar (1993), The meteorological environment of the tropospheric ozone maximum over the tropical south Atlantic ocean, *J. Geophy. Res.*, *98*, 10,621–10,641.

Krishnamurti, T. N., et al. (1996), Passive tracer transport relevant to the TRACE-A experiment, *J. Geophy. Res.*, *101*, 23,889–23,907.

Levy, H., II, P. S. Kasibhatla, W. J. Moxim, A. A. Klonecki, A. I. Hirsch, S. J. Oltmans, and W. L. Chameides (1997), The global impact of human activity on tropospheric ozone, *Geophys. Res. Lett.*, *24*, 791–794.

Lorenc, A. C., et al. (2000), The Met. Office global three-dimensional variational data assimilation scheme, *Q. J. R. Meteorol. Soc.*, *126*, 2992–3012.

McCormick, M. P. (1987), SAGE II: An overview, *Atmos. Sci. Rev.*, *7*, 319–326.

Moxim, W. J., and H. Levy II (2000), A model analysis of the tropical South Atlantic Ocean tropospheric ozone maximum: The interaction of transport and chemistry, *J. Geophy. Res.*, *105*, 17,393–17,415.

Newell, R. E., J. W. Kidson, D. G. Vincent, and G. J. Boer (1974). *The General Circulation of the Tropical Atmosphere*, 371 pp., MIT Press, Cambridge, Mass.

Olson, J. R., J. Fishman, V. W. J. H. kirchhoff, D. Nganga, and B. Cros (1996), Analysis of the distribution of ozone over the southern Alantic region, *J. Geophy. Res.*, *101*, 24,083–24,094.

Peixoto, J. P., and A. H. Oort (1992), *Physics of Climate*, 520 pp., Am. Inst. of Phys., New York.

Peters, W., M. Krol, E. Dentener, A. M. Thompson, and J. Lelieveld (2002), Chemistry-transport modeling of the satellite observed distribution of tropical tropospheric ozone, *Atmos. Chem. Phys.*, *2*, 103–120.

Pickering, K. E., et al. (1996), Convective transport of biomass burning emissions over Brazil during TRACE A, *J. Geophys. Res.*, *101*, 23,993–24,012.

Postel, A. P., and M. H. Hitchman (1999), A climatology of Rossby wave breaking along the subtropical tropopause, *J. Atmos. Sci.*, *56*, 359–373.

Rosenlof, K. H., A. F. Tuck, K. K. Kelly, J. M. Rissell III, and M. P. McCormick (1997), Hemispheric asymmetries in water vapor and inferences about transport in the lower stratosphere, *J. Geophy. Res.*, *102*, 13,213–13,234.

Sauvage, B., V. Thouret, J.-P. Cammas, F. Gheusl, G. Athier, and P. Nédélec (2004), Tropospheric ozone over equatorial Africa: Regional aspects from the MOZAIC data, *Atmos. Chem. Phys. Discuss.*, *4*, 3285–3332.

Schubert, S., C.-K. Park, W. Higgins, S. Moorthi, and M. Suarez (1990), An atlas of ECMWF analyses (1980–1987) part I—First moment quantities, *Tech. Memo. 100747*, NASA, Washington, D. C.

Shiotani, M. (1992), Annual, quasi-biennial and El Niño-Southern Oscillation (ENSO) timescale variations in Equatorial total ozone, *J. Geophy. Res.*, *97*, 7625–7634.

Suhre, K., J.-P. Cammas, P. Nédelec, R. Rosset, A. Marenco, and H. G. J. Smit (1997), Ozone-rich transients in the upper equatorial Atlantic troposphere, *Nature*, *388*, 661–663.

Swinbank, R., and A. O'Neill (1994), A stratosphere-troposphere data assimilation system, *Mon. Weather Rev.*, *122*, 686–702.

Thompson, A. M. (2003), Tropical tropospheric ozone: A perspective on photochemical and dynamical interactions from observations in the past five years, *IGAC Newsl.*, *28*, 6–11.

Thompson, A. M., et al. (1996), Where did tropospheric ozone over southern Africa and the tropical Atlantic come from in October 1992?: Insights from TOMS, GTE/TRACE-A and SAFARI-92, *J. Geophy. Res.*, *101*, 24,251–24,278.

Thompson, A. M., B. G. Doddridge, J. C. White, R. D. Hudson, W. T. Luke, J. E. Johnson, B. J. Johnson, S. J. Oltmans, and R. Walter (2000), A tropical Atlantic paradox: Shipboard and satellite views of a tropospheric ozone maximum and wave-one in January-February 1999, *Geophy. Res. Lett.*, *27*, 3317–3320.

Thompson, A. M., J. C. White, R. D. Hudson, H. Guo, J. R. Herman, and M. Fujiwara (2001), Tropical tropospheric ozone and biomass burning, *Science*, *291*, 2128–2132.

Thompson, A. M., et al. (2003), Southern Hemisphere Additional Ozonesonde (SHADOZ) 1998–2000 tropical ozone climatology: 2. Tropospheric variability and the zonal wave-one, *J. Geophy. Res.*, *108*(DX), 8241, doi:10.129/2002JD002241.

Thompson, A. M., J. C. Witte, S. J. Oltmans, and F. J. Schmidlin (2004), SHADOZ-A tropical ozonesonde-radiosonde network for the atmospheric community, *Bull. Am. Meteorol. Soc.*, *85*, 1549–1564.

Trenberth, K. E. (1992), Global analyses from ECMWF and atlas of 1000 to 10 mb circulation statistics, *NCAR TN-373+STR*, Natl. Cent. for Atmos. Res., Boulder, Colo.

Tyson, P. D., M. Garstang, A. M. Thompson, P. D'Abreton, R. D. Diab, and E. V. Browell (1997), Atmospheric transport and photochemistry of ozone over central Southern Africa during the Southern Africa Fire-Atmosphere Research Initiative, *J. Geophy. Res.*, *102*, 10,623–10,635.

Wang, P.-H. (1994), SAGE II tropospheric measurement frequency and its meteorological implication, in *Seventh Conference on Satellite Meteorology and Oceanography*, pp. J15–J18, Am. Meteorol. Soc., Boston.

Wang, P.-H., M. P. McCormick, L. P. Poole, W. P. Chu, G. K. Yue, G. S. Kent, and K. M. Steens (1994), Tropical high cloud characteristics derived from SAGE II extinction measurements, *Atmos. Res.*, *34*, 53–83.

Wang, P.-H., P. Minnis, M. P. McCormick, G. S. Kent, and K. M. Skeens (1996), A 6-year climatology of cloud occurrence frequency from SAGE II observations (1985–1990), *J. Geophy. Res.*, *101*, 29,407–29,429.

Wang, P.-H., D. Rind, C. R. Trepte, G. S. Kent, G. K. Yue, and K. M. Skeens (1998a), An empirical model study of the tropospheric meridional circulation based on SAGE II observations, *J. Geophy. Res.*, *103*, 13,801–13,818.

Wang, P.-H., D. M. Cunnold, J. M. Zawodny, R. B. Pierce, J. R. Olson, G. S. Kent, and K. M. Skeens (1998b), Seasonal ozone variations in the isentropic layer between 330 and 380 K as observed by SAGE II: Implications of extratropical cross-tropopause transport, *J. Geophy. Res.*, *103*, 28,647–28,659.

Wang, Y. H., D. J. Jacob, and J. A. Logan (1998c), Global simulation of tropospheric O_3-NO_x-hydrocarbon chemitry, 3, origin of tropospheric ozone and effects of non-methane hydrocarbon, *J. Geophys. Res.*, *103*, 10,757–10,768.

Wang, P.-H., R. E. Veiga, L. B. Vann, P. Minnis, and G. S. Kent (2001), A further study of the method for estimation of SAGE II cloud occurrence, *J. Geophy. Res.*, *106*, 12,603–12,613.

Wang, H. J., D. M. Cunnold, L. W. Thomason, J. M. Zawodny, and G. E. Bodeker (2002), Assessment of SAGE version 6.1 ozone data quality, *J. Geophys. Res.*, *107*(D23), 4691, doi:10.1029/2002JD002418.

Wang, P.-H., P. Minnis, B. A. Wielicki, T. Wong, R. D. Cess, M. Zhang, L. B. Vann, and G. S. Kent (2003), Characteristics of the 1997/1998 El Niño cloud distributions, *J. Geophys. Res.*, *108*(D1), 4009, doi:10.1029/2002JD002501.

Webster, P. J. (1983), Large-scale structure of the tropical atmosphere, in *Large-Scale Dynamical Processes in the Atmosphere*, edited by B. J. Hoskins and P. Pearce, pp. 235–276, Elsevier, New York.

Wennberg, P. O., et al. (1998), Hydrogen radicals, Nitrogen radicals, and the production of O_3 in the upper troposphere, *Science*, *279*, 49–53.

Zachariasse, M., P. F. J. van Velthoven, H. G. J. Smit, J. Lelieveld, T. K. Mandal, and H. Kelder (2000), In fluence of stratosphere-troposphere exchange on tropospheric ozone over the tropical Indian Ocean during the winter monsoon, *J. Geophy. Res.*, *105*, 15,403–15,416.

Zachariasse, M., H. G. J. Smit, P. F. J. van Velthoven, and H. Kelder (2001), Cross-tropopause and interhemispheric transports into the tropical free troposphere over the Indian Ocean, *J. Geophy. Res.*, *106*, 28,441–28,452.

J. Fishman, Science Directorate, NASA Langley Research Center, MS 401A, Hampton, VA 23681-2199, USA. (jack.fishman@nasa.gov)

V. L. Harvey, Laboratory for Atmospheric and Space Physics, University of Colorado, UCB 392, Boulder, CO 80309-0392, USA. (lynn.harvey@lasp.colorado.edu)

M. H. Hitchman, Atmospheric and Oceanic Sciences, University of Wisconsin, 1225 West Dayton Street, Madison, WI 53706, USA. (matt@aos.wisc.edu)

P.-H. Wang, Science and Technology Corporation, 10 Basil Sawyer Drive, Hampton, VA 23666, USA. (p.wang@larc.nasa.gov)